MOLECULAR DYNAMICS (MD) THERMAL SIMULATIONS OF MOLECULAR BRIDGING ACROSS THE CATHODE-SEPARATOR INTERFACE IN LI-ION CELL

By,

Abhijeet S. Dhakane

Presented to the Faculty of the Graduate School of
The University of Texas at Arlington
in partial fulfillment of the requirements
for the degree of
MASTER OF SCIENCE IN MECHANICAL ENGINEERING

THE UNIVERSITY OF TEXAS AT ARLINGTON
August 2019

ACKNOWLEDGEMENT

I would like to express my sincere gratitude to Dr. Ankur Jain for giving me an excellent opportunity to work in his group for past 1.5 year. His help me in developing a mindset that is needed for doing research is highly appreciated. I would like to thank my committee members Dr. Hyejin Moon and Dr. Alan Bowling for reviewing my work.

I want to pay my due respect to Dr. Vikas Varshney (AFRL) for sharing his thoughts and suggestions for the molecular dynamics simulations. I would like to thank Dr. Hendrik Heinz for sharing the force-field parameters and Dr. Luis for helping me to model the system for simulations.

All these works would not have been made possible with the support of all my lab members Darshan,Amir, Mohammad, Swapnil, Aditya, Dhananjay and Hardik for insightful discussions. Last but not the least I thank my mom dad and all other family members for their constant support.

August 14, 2019

ABSTRACT

MOLECULAR DYNAMICS (MD) THERMAL SIMULATIONS OF MOLECULAR BRIDGING ACROSS THE CATHODE-SEPARATOR INTERFACE IN LI-ION CELL

Abhijeet S. Dhakane, MS

The University of Texas at Arlington

Supervising Professor: Dr. Ankur Jain

While Li-ion cells show outstanding electrochemical performance, their poor thermal transport characteristics results in reduced performance as well as significant safety concerns. The heterogeneous interface between cathode and separator plays a vital role in the dissipation of heat within a Li-ion cell. Previous studies showed that the cathode-separator interfacial thermal resistance contributes around 88% of total thermal resistance within the cell. In this research, thermal conductance across the cathode-separator interface is calculated using molecular dynamics simulations. Thermal transport in a pristine heterogeneous interface as well as interfaces functionalized with monolayers of APTES, nBTMS and MPTMS molecules is studied. The impact of molecular density and external pressure on the interfacial thermal transport is

studied. It was observed that interfacial functionalization results in significant improvement in interfacial thermal conductance, which is consistent with past experimental data. Molecular dynamics simulations presented here help validate past experimental measurements. Using 20 MPTMS molecules, 174% improvement in thermal conductance was observed compared to bare interface.2X improvement in 20 molecules of nBTMS by applying 100 bar pressure was observed compared to non-pressured of same system. These results highlight the key role of the cathode-separator interface in thermal transport within the cell, as well as the significant impact of functionalizing the interface to mitigate poor thermal transport in the Li-ion cell.

TABLE OF CONTENTS

LIST OF FIGURES

LIST OF TABLES

CHAPTER 1

INTRODUCTION

Li-ion cells are used widely in a large number of energy storage applications, including electric vehicles, consumer electronics, renewable energy storage, etc. [1,2]. High energy storage density is a key advantage of Li-ion cells compared to other energy storage technologies. Energy storage in a Li-ion cell occurs via intercalation and de-intercalation of Li ions between a cathode material, typically made of a Li salt such as $LiCoO_2$, $LiFePO_4$, etc. and an anode, typically made of graphite [3]. The anode and cathode are typically separated by a polymer-based separator. A roll or multiple folds of cathode-separator-anode-separator sheets are packed tightly into cylindrical or prismatically shaped cells. A large number of such cells are electrically connected with each other with modules and battery packs.

Poor thermal transport in Li-ion cells and battery packs is widely recognized to be a key technological concern that limits the use of Li-ion cells [4,5]. Overheating in Li-ion cells, often caused by poor thermal conductance within the cell, results in large temperature rise in the cell. Above a certain threshold, high cell temperature causes increased rate of heat generation due to exothermic decomposition processes, which in turn raises the cell temperature further. This positive feedback phenomena, called thermal runaway is unsustainable and results in catastrophic failure and fire [6,7].

It is clearly desirable to understand and enhance thermal transport within a Li-ion cell for improved safety and performance. While a number of thermal management strategies have been investigated for external thermal management of Li-ion cells [4,8,9,10], thermal transport within

the cell is known to be a rate-limiting step [7,11,12,13] and therefore must be fully understood and optimized. In addition to being orthotropic, overall thermal conductivity of Li-ion cells has been measured to be very poor, of the order of 0.2-0.6 W/mK [14,15]. Past work has demonstrated multiple benefits of improving thermal conductivity of the cell, including reduced likelihood of thermal runaway [12], increased discharge rate capability [11], increased energy storage density through reduced requirement for external thermal management [16], etc.

Given that most constituent materials within a Li-ion cell have reasonably high thermal conductivity [13,17], the overall poor thermal conductivity indicates dominance of interfacial thermal resistance in determining overall rates of heat flow [13]. Recently reported measurements show that interfacial thermal resistance at the cathode-separator interface constitutes about 90% of overall thermal resistance within a Li-ion cell [12]. Using acoustic mismatch theory [18], such high resistance has been explained on the basis of high mismatch in speeds of sound in separator and cathode materials [13], although a detailed explanation using more fundamental thermal transport simulations is missing.

Further, measurements have shown that interfacial thermal transport between the cathode and separator can potentially be improved through molecular bridging between the two materials [13]. A monolayer of aminosilane between cathode and separator has been shown to result in 3X reduction in measured thermal contact resistance [13]. This is consistent with other experiments that report similar thermal enhancement with the use of molecular bridging between other material pairs [19,20]. However, the literature specific to interfacial thermal transport in Li-ion cells is rather sparse. For example, it is not clear which molecules are most suitable for the specific materials that constitute the cathode and separator in a Li-ion cell. Given the large number of potential molecules to be used as molecular bridges, it is important to develop computation tools

to characterize thermal performance of various molecules of enhanced interfacial thermal transport. Such a tool will help downselect candidate molecules, which can then be characterized experimentally. Such a capability is particularly important in the context of Li-ion cells because of the complex and coupled nature of thermal and electrochemical transport in a Li-ion cell, as well as due to the time-consuming nature of experiments needed to establish long-term reliability and safety of any material changes within the cell.

Till now most of the literature given the information of the electrochemical transport in point of view of Li-ion by using the abinitio techniques. On contrary there were limited theoretical as well classical atomistic/molecular study had been performed primarily focused on the thermal transport properties due to unavailability of proper force-fields for the Li-oxide compounds.

REFRENCES:

[1] Cahill, D. G. et al. Nanoscale thermal transport. 793, (2009).

[2] B. Scrosati, J. Garche, *J. Power Sources* 9 (2010) 2419e2430.

[3] G. Karimi, X. Li, *Int. J. Energy Res.* 37 (2013) 13e24.

[4] Shah, K., Vishwakarma, V., Jain, A., 'Measurement of multiscale thermal transport phenomena in Li-ion cells: A review,' ASME J. Electrochem. *Energy Conversion & Storage (Special Issue on Multiphysics Coupling in Energy Storage),* 13, pp. 030801:1-13, 2016. (1 = Equal Contribution).

[5] T.M. Bandhauer, S. Garimella, T. Fuller, *J. Electrochem. Soc.* 158 (2011) R1-R25.

[6] R. Spotnitz, J. Franklin, *J. Power Sources* 113 (2003) 81–100.

[7] Shah, K., Chalise, D., Jain, A., 'Experimental and theoretical analysis of a method to predict thermal runaway in Li-ion cells,*' J. Power Sources,* 330, pp. 167-174, 2016.

[8] Anthony, D., Wong, D., Wetz, D., Jain, A., 'Improved thermal performance of a Li-ion cell through heat pipe insertion,' *J. Electrochem. Soc.,* 164, pp. A961-967, 2017.

[9] Jin, L.W., Lee, P.S., Kong, X.X., Fan, Y. and Chou, S.K., 2014, "Ultra-thin minichannel LCP for EV battery thermal management," *Applied Energy,* 113, pp.1786-1794.

[10] Xu, X.M. and He, R., 2013, "Research on the heat dissipation performance of battery pack based on forced air cooling*," J. Power Sources*, 240, pp.33-41.

[11] Shah, K., Drake, S.J., Wetz, D.A., Ostanek, J.K., Miller, S.P., Heinzel, J.M., Jain, A., 'An experimentally validated transient thermal model for cylindrical Li-ion cells,*' J. Power Sources*, 271, pp. 262-268, 2014.

[12] Esho, I., Shah, K., Jain, A., 'Measurements and modeling to determine the critical temperature for preventing thermal runaway in Li-ion cells,' *Appl. Therm. Eng.,* 145, pp. 287-294, 2018.

[13] . Vishwakarma, V., Waghela, C., Wei, Z., Prasher, R.*, Nagpure, S.C., Li, J., Liu, F., Daniel, C., Jain, A., 'Heat transfer enhancement in a Lithium-ion cell through improved material-level thermal transport,' *J. Power Sources*, 300, pp. 123-131, 2015.

[14] Drake, S., Wetz, D.A., Ostanek, J.K., Miller, S.P., Heinzel, J.M., Jain, A., 'Measurement of anisotropic thermophysical properties of cylindrical Li-ion cells,' *J. Power Sources*, 252, pp. 298-304, 2014.

[15] http://dx.doi.org/10.1016/j.jpowsour.2014.02.079

[16] Chalise, D., Shah, K., Prasher, R., Jain, A., 'Conjugate heat transfer analysis of thermal management of a Li-ion battery pack,' *ASME J. Electrochem. Energy Conversion & Storage*, 15, pp. 011008:1-8, 2018.

[17] J. Cho, M.D. Losego, H.G. Zhang, H. Kim, J. Zuo, I. Petrov, D.G. Cahill, P.V. Braun, *Nature Communications* 5 (2014) 1-6.

[18] E.T. Swartz, R.O. Pohl, *Rev. Modern Phys.,* 61 (1989) 605.

[19] P.J. O'Brien, S. Shenogin, J. Liu, P.K. Chow, D. Laurencin, P.H. Mutin, M. Yamaguchi, P. Keblinski, G. Ramanath, *Nature Mater*. 12 (2012) 118-122.

[20] S. Kaur, N. Raravikar, B.A. Helms, R. Prasher, D.F. Ogletree, *Nature Communications* 5 (2014) 3082:1-8.

CHAPTER 2

MOLECULAR DYNAMICS

2.1 Overview

Experimental techniques were developed for carrying out measurement in thermal and optical domains to evaluate the properties of interest such as thermal conductivity etc. [1] Those techniques were well optimized to determine the transport properties to find the transport properties across interfaces as well [2,3]. Well-developed theoretical models like AMM and DMM were sometimes difficult to get in agreement with the experimental observations as the interfacial properties highly deviates according to the surround environment and the situations at the time of the experiments. To evolve the interfacial properties efficiently, more robust theoretical models like molecular/atomistic simulations came into the role around 1950's over its development in period of 4-5 decades those models were well optimized to predict the intricate transport properties and provides a better overall microscopic picture at the interface transport properties.

Molecular Dynamics evolve earlier in the 1950's. Molecular dynamics basically traces the trajectory of the particles over the period of time by solving Newton's law of motions. Interatomic potential functions were used to predict the motion between the atoms [4]. Interatomic potential function i.e. mathematical formulation for deciding the atom-atom interactions were play key role in the evaluating the properties and decides the quality of the values of the properties. Till now software's like LAMMPS, NAMD etc[5]. were well optimized codes available with the most of compatible interatomic potentials for modelling different atoms and molecules. For this study we have used LAMMPS software for performing all MD simulations.

LAMMPS provide flexible capability to perform simulations in different domains such as thermal transport, fluid flow, phase transformations of the fluids and crystals to deduce thermal conductivity, viscosity, various phases of the matter etc. properties of the system. Method such as equilibrium dynamics and Non-equilibrium dynamics were well used to determine the thermal transport properties across the interface of the heterogeneous system.

2.1.1 Equilibrium molecular dynamics (EMD):

Equilibrium Molecular Dynamics commonly known as Green-Kubo formulations, it calculates the thermal transport properties by using the fluctuations and dissipations from the system. As this method is more reliable to calculate the system of small sizes, properties were not much deviate with the system size. Simulations performed using EMD for the silicon thermal transport properties were well consistent with the experimental data [6]. This method is effective for a homogeneous system but was not as effective to predict the interfacial thermal transport properties.

2.1.2 Non equilibrium molecular dynamics (NEMD):

Comparative to the EMD this method has a similar analogy as used in the experiments to calculate the thermal transport properties, which can be use in two ways by providing constant heat current and measure the temperature gradient across interface or vice versa. While performing NEMD energy is constantly added and subtracted in a way to maintain the hot and cold reservoirs. Over the period of time steady state and temperature gradient established in a system. Using the Fourier's law, thermal properties for the system predicted. For this study we have used the NEMD approach to evaluate the thermal transport properties across the cathode-separator interface. Approach of classical atomistic simulations will provide an insightful microscopic picture at the

interface which will eventually help to study the various factors affecting the interfacial transport properties especially thermal.

2.2 Simulation Details:

The commonly used material for the Li-ion battery, among $LiCoO_2$ (cathode) and the polyethylene (separator) selected for the interfacial thermal transport study. For initial part $LiCoO_2$, orthogonal cell of size (~ 29 X 28 X 70 Å) was created in Material Studio 7.0[7]. Separator, amorphous polyethylene with 40 ($-CH_2-$) monomers of 47 chains were built in Material Studio 7.0 using amorphous polymer builder of similar size. Consistent valence force field (CVFF)[8] was used, as it able to reproduce the required properties.

Table 2.1 $LiCoO_2$ CVFF parameters

I. Nonbond	**Atomic charge (e)**	**σ (pm)**	**ε (kcal·mol^{-1})**
Li	+0.62	173	0.04
O	-0.80	345	0.15
Co	+0.98	450	0.04
II. Bond	**$r_{0,\,ij}$ (pm)**		**K_r (kcal·mol^{-1}·Å^{-2})**
Co-O	239		118
III. Angles	**$\theta_{0,\,ijk}$ (°)**		**K_θ (kcal·mol^{-1}·rad^{-2})**
∠Co-O-Co	98		85
∠O1-Co-O1	98		85
∠O2-Co-O2	98		85
∠O1-Co-O2	84.5		0

Therefore, among all CVFF parameters were selected to model $LiCoO_2$, amorphous polyethylene, and functionalize molecules. The parameters for $LiCoO_2$ were recently developed in Interface force field (IFF) 1 -CVFF represent chemical bonding with experimental lattice geometry, density, mechanical properties and cleavage energy (DFT). Partial charge calculations performed using Discover program in Material Studio 7.0. LAMMPS [5] package was used to perform all the simulations. Using PPPM (Particle-Particle-Particle Mesh) with energy tolerance of 1×10^{-5} long-range electrostatic interactions considered and van der Waals interactions, a distance cutoff of 12.0 Å used for all the simulations.

Both structures brought closed enough to form an interface, for mimic bulk like system periodic boundary condition employed in all three orthogonal directions. Resultant structure minimized with conjugate gradient algorithm followed by heating at 300 K, employing NVT canonical ensemble for 100 ps, followed by NPT (isothermal−isobaric) ensemble to equilibrate the pressure and density for 100 ps with independent barostats along the orthogonal x-, y-, and z-directions. By confirming the minimum energy fluctuations, system is said to be equilibrated. All simulations were performed with 1fs time step for the integrations while performing equilibration. At the start of the thermal interface calculations, all simulations equilibrated with 100 ps NVT ensemble.

2.2.1 Functionalize the interface:

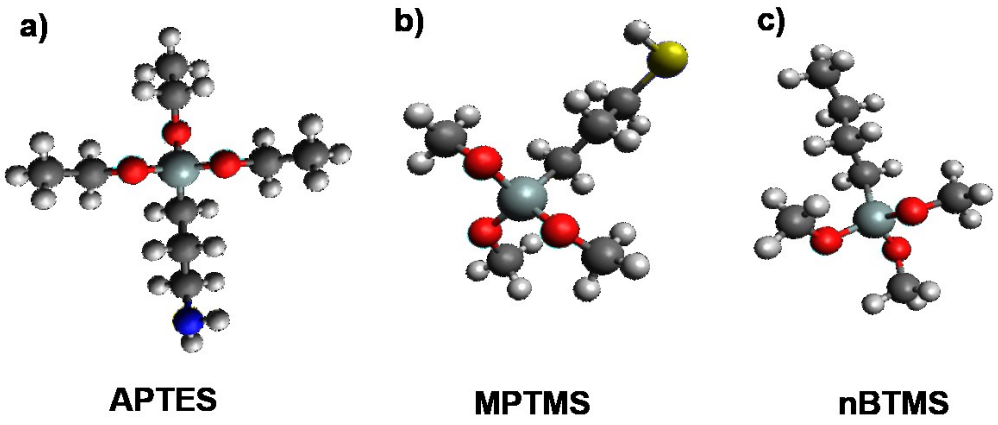

Figure 2.1 Shows the MNL molecules used to functionalize the cathode-separator interface. a) APTES [3-Aminopropyl triethoxysilane] b) MPTMS [3- Mercaptopropyl trimethoxysilane] c) nBTMS [n-Butyl trimethoxysilane]. [Colour code Si-Cyan, C- Gray, H-White, O-Red, N-Blue, S-Yellow]

The unique capability of alkylsilanes are known to self-assemble on the metal oxide surface. These characteristics widely used to adjust the surface morphology leads to alter wetting and transport properties [9,10,11,12]. Molecule APTES (3-Aminopropyl) triethoxysilane, nBTMS (n-butyl) trimethoxysilane, MPTMS (3-mercaptopropyl) triethoxysilane one of the alkylsilanes molecules selected for the functionalization of an interface, experimental evidence showed that the reduction in the interfacial thermal resistance [13,14,15,16]. Having varying functional sites on the other ends. Consistent valence force field (CVFF) employed for the all MNL molecules. Varying the number of molecules at the interface, comparative interfacial thermal transport study performed.

2.2.2 Effect of pressure:

To avoid the voids in the system especially for amorphous polyethylene and MNL molecules. System was relaxed using NPT ensemble with 100 bar pressure in the z-direction for 1 ns followed by 500ps NPT and NVE ensemble to ensure the system reached at equilibrium with minimum

percentage of void after this relaxation cell size in z-direction were decreased by ~3-4 Å which was also result in increased areal density.

2.2.3 NEMD

Interfacial thermal conductance calculation across the $LiCoO_2$ and amorphous polyethylene with and without functionalization were performed using Nonequilibrium molecular dynamics (NEMD) simulations from an orthogonal structure based on Fourier's law of heat conduction. As shown in the given figure. End edges of the orthogonal slab (~ 0.5 nm) were fixed, adjacent 1 nm bins were set to be as hot and cold reservoir. By applying temperature rescaling algorithm reservoirs maintained at 350K and 250K respectively. To conserve the energy of the total system and eventually establish a steady state thermal gradient between two reservoirs NVE (micro-canonical) ensemble employed in non-fixed region. Energy was continuously added and subtracted from the hot and cold reservoirs to maintain at the specified temperatures. Temperature profile was calculated in the elongated direction of the orthogonal box by dividing it into (~ 2 Å) chunks. Temperature profiles of each chunk calculated by equating the total kinetic energy of the chunk with the temperature of each chunk was calculated using following equation.

$$\frac{1}{2}\Sigma m_i v_i^2 = \frac{3}{2}k_b T_i$$

Where m_i, v_i and T_i will be the mass, velocity and temperature of the atoms in the i^{th} bin, k_b is a Boltzmann constant. Solving above equation will give a temperature of the i^{th} bin.

Steady state thermal gradient was established in the system over the period of time, in the elongated direction. However, at the interface due to heterogeneity of the molecular system abrupt temperature drop observed. Following equation was used to calculated the interfacial thermal conductance.

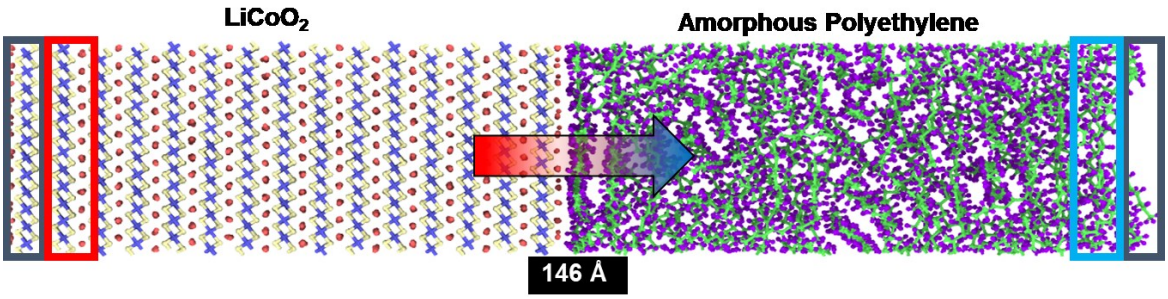

Figure 2.2 Shows $LiCoO_2$ and a-PE interface without MNL , hot reservoir (red rectangle) and cold reservoir (blue rectangle) maintained at 350K and 250K respectively of length ~1 nm, edges of similar size having fixed boundary

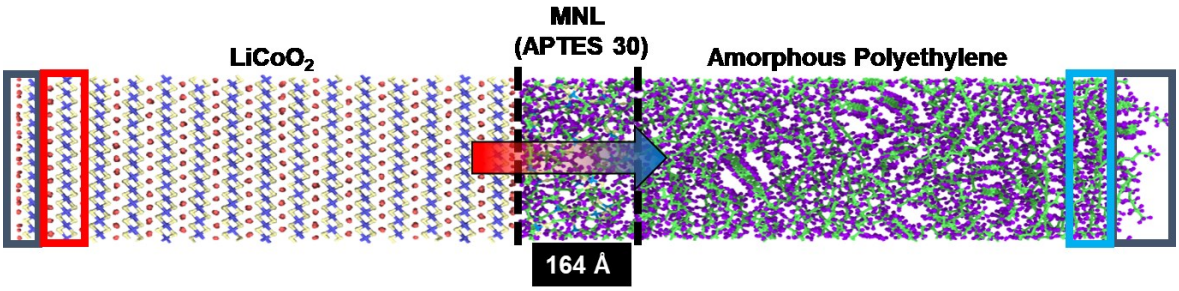

Figure 2.3 Shows $LiCoO_2$ and a-PE interface with MNL (APTES 30 molecules), hot reservoir (red) and cold reservoir (blue) maintained at 350K and 250K respectively of length ~1 nm, edges of similar size having fixed boundary

$$\lambda = \frac{\dot{Q}}{\Delta T}$$

Where λ, Q, T are thermal conductance, heat flux per unit area and temperature drop at interface respectively. Heat flux per unit area calculated by taking average absolute slope of energy, which added and subtracted to maintain the hot and cold reservoir temperature and divided it by the interfacial area. Simulation was carried out for 5 ns to achieve steady state and data collection of temperature profiles which was used to calculate heat flux and gradient in temperature profile.

REFERENCES:

[1] Luo, T. and Chen, G., Nanoscale heat transfer - from computation to experiment,"*Physical Chemistry Chemical Physics*, Vol. 15, No. 10, jan 2013, pp. 3389.

[2] Cahill, D. G., Ford, W. K., Goodson, K. E., Mahan, G. D., Majumdar, A., Maris,H. J., Merlin, R., and Phillpot, S. R., Nanoscale Thermal Transport," *Journal of Applied Physics,* Vol. 93, No. 2, Jan. 2003, pp. 793.

[3] Barnes, L. J. and Dillinger, J. R., \Thermal resistivity at Pb-Cu and Sn-Cu interfaces between 1.3 and 2.1 K*," Physical Review*, Vol. 141, No. 2, jan 1966, pp. 615

[4] Allen, M. and Tildesley, D., *Computer Simulation of Liquids*, Oxford, 1987.

[5] Plimpton, S. Fast Parallel Algorithms for Short-Range Molecular Dynamics. *J. Comput. Phys. 1995*, 117,1−19.

[6] Volz, S. G. and Chen, G., \Molecular-dynamics simulation of thermal conductivity of silicon crystals," *Physical Review B*, Vol. 61, No. 4, 2000, pp. 2651-2656.

[7] *Dassault Systèmes BIOVIA, Material Studio, Release 2017,* San Diego: Dassault Systèmes, 2019.

[8] Heinz, H.; Lin, T.-J.; Kishore Mishra, R.; Emami, F. S., Thermodynamically consistent force fields for the assembly of inorganic, organic, and biological nanostructures: the INTERFACE force field. *Langmuir : the ACS journal of surfaces and colloids 2013*, 29 (6), 1754-1765.

[9] Onclin S.; Ravoo B. J.; Reinhoudt D. N. Engineering Silicon Oxide Surfaces Using Self-Assembled Monolayers. Angew. *Chem., Int. Ed. 2005*, 44, 6282–630410.1002/anie.200500633

[10] Cappelletti G.; Ardizzone S.; Meroni D.; Soliveri G.; Ceotto M.; Biaggi C.; Benaglia M.; Raimondi L. Wettability of Bare and Fluorinated Silanes: A Combined Approach Based on Surface Free Energy Evaluations and Dipole Moment Calculations. *J. Colloid Interface Sci. 2013,* 389, 284–29110.1016/j.jcis.2012.09.008.

[11] Meroni D.; Ardizzone S.; Cappelletti G.; Ceotto M.; Ratti M.; Annunziata R.; Benaglia M.; Raimondi L. Interplay between Chemistry and Texture in Hydrophobic TiO_2 Hybrids. *J. Phys. Chem. C 2011,* 115, 18649–1865810.1021/jp205142b.

[12] Herzer N.; Haensch C.; Hoeppener S.; Schubert U. S. Orthogonal Functionalization of Silicon Substrates using Self-Assembled Monolayers. *Langmuir 2010,* 26, 8358–836510.1021/la9047837.

[13] Vishwakarma, V. *et al.* Heat transfer enhancement in a lithium-ion cell through improved material-level thermal transport. *J. Power Sources* **300**, 123–131 (2015).

[14] O'Brien, P. J. *et al.* Bonding-induced thermal conductance enhancement at inorganic heterointerfaces using nanomolecular monolayers. *Nat. Mater.* **12**, 118–122 (2013).

[15] Losego, M. D., Grady, M. E., Sottos, N. R., Cahill, D. G. & Braun, P. V. Effects of chemical bonding on heat transport across interfaces. *Nat. Mater.* **11**, 502–6 (2012).

[16] Varshney, V.; Roy, A. K.; Michalak, T. J.; Lee, J.; Farmer, B. L. Effect of Curing and Functionalization on the Interface Thermal Conductance in Carbon Nanotube−Epoxy Composites. *JOM 2013,* 65, 140−146.

CHAPTER 3

RESULTS

3.1 Interfacial Thermal Conductance without functionalization:

By performing NEMD simulation for the initial configuration shown in fig (2.2). It was possible to predict the interfacial thermal conductance at the interface. Following were the graphs of energy added and subtracted from the cold and hot thermostats respectively after taking absolute average of both heat currents in the system has been calculated as the area of the xy-plane known beforehand as the heat current was only flowing through the elongated direction i.e., in this case, heat flux for the same calculated. For this last 2 ns reading were taken as the system have minimum fluctuations and reached the steady-state.

From fig. (3.1) , it was conceivable to evaluate the cathode side have the very lower slope, as a result, have more thermal conductivity value, on the contrary, the separator side the amorphous polyethylene has a maximum slope so as the lower thermal conductivity of 0.9 W/mK as per expectations. As a result, a temperature drops of 17.7 K at the interface as a result of the phonon velocity mismatch. Further, by dividing the heat flux of 221 MW/m^2 with the temperature drops i.e., 17.7 K, interfacial thermal conductance for the system of 125 MW/m^2K found out. This result is taken as the baseline to compare the percentage increase/drop in functionalize and with pressure systems.

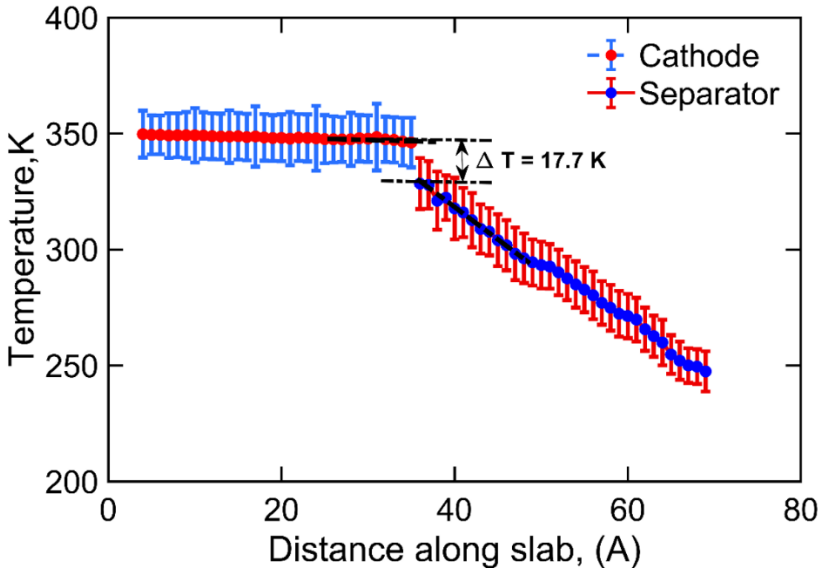

Figure 3.1 Temperature profile of the pristine cathode-separator interface.

3.2 Effect of functionalization:

System of varying number of molecules 10/20/30 with functionalize molecules APTES, MPTMS and nBTMS was made to evaluate the effect of number of molecules and functionalization sites of the molecules of the $LiCoO_2$ and amorphous polyethylene.

3.2.1 Effect of APTES Molecules on cathode-separator interface:

In this system APTES molecules i.e., (3 – Aminopropyl triethoxy silane) were used. APTES molecules have two functional sites on there each end one was silane group and other end with amine group. Previous studies evident that the silane group is attractive towards the oxide group while the amine group have more affinity towards the organic molecules. APTES molecules in the experiments resulted the 3X improvement in the interfacial thermal resistance. From the below results, for 10 APTES molecules interfacial thermal conductance %increase with respect to normal was around 138% by increase in 10 more molecules it got slightly drop to 89% and

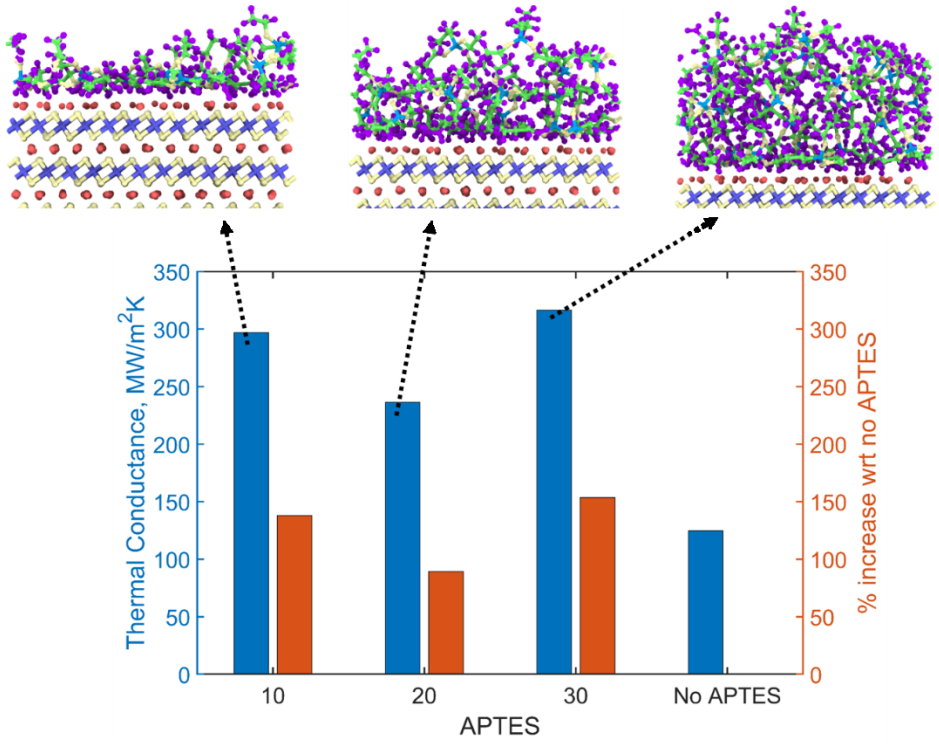

Figure 3.2 Shows the comparative results with increase in the number of molecules 10/20/30 APTES (blue-right) while the (orange-left) represent the percentage increase in the interfacial thermal conductance with respect to the pristine interface have no APTES molecules.

Table 3.1 APTES system thermal properties from MD simulations.

	APTES 10	APTES 20	APTES 30
Heat Flux (W/m^2)	1986936343	1759134724	2143866347
Temperature drop at interface (K)	6.69181	7.443624	6.772893
Interfacial Thermal Conductance (W/m^2K)	296920624.2	236327731.1	316536269.5

again rises to 154% with 30 molecules. Results shown was not have a linear trend. Mechanisms of this improvement elucidated by taking the effect of end group affinities towards the $LiCoO_2$ and amorphous polyethylene. Amine groups were well attracted towards the organic group such as amorphous polyethylene which is essentially a $–[CH_3-]$ group while the silane group towards the $LiCoO_2$, so facilitating the covalent interfacial bonding as earlier with no APTES molecules had a weak Van der Waals bonding, accounting the overall affinity from both the end groups provides strong interfacial bonding results in improvement in the interfacial contact that

eventually leads in the good strength and a very good medium for the thermal transport and therefore interfacial thermal conductance has been improved.

3.2.2 Effect of nBTMS Molecules on cathode-separator interface

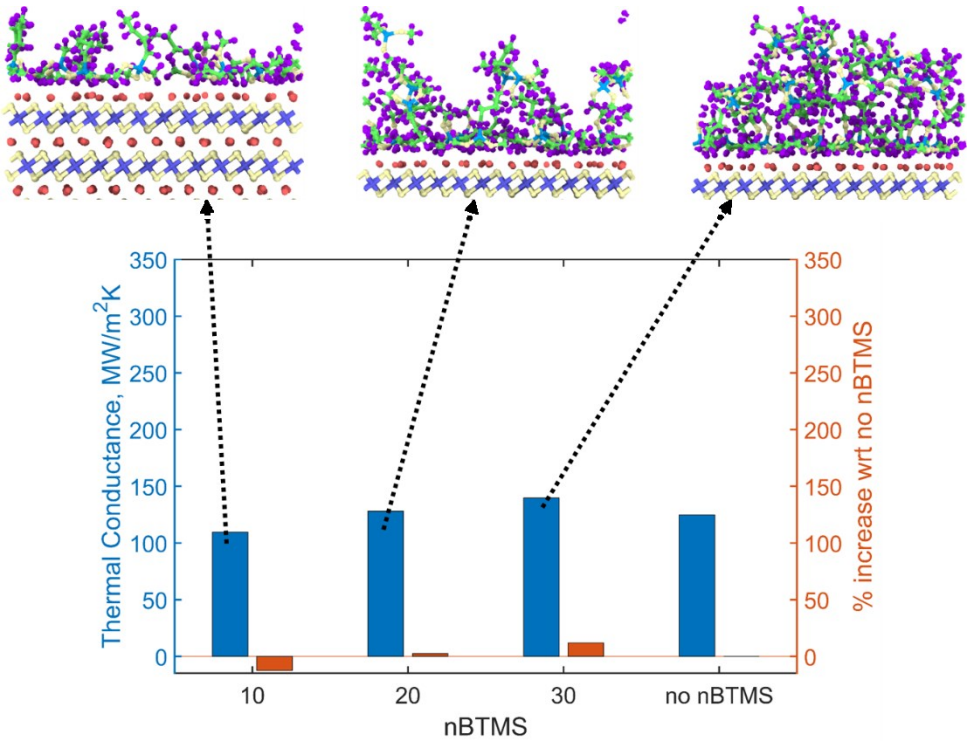

Figure 3.3 Shows the comparative results with increase in the number of molecules 10/20/30 nBTMS (blue-right) while the (orange-left) represent the percentage increase in the interfacial thermal conductance with respect to the pristine interface have no nBTMS molecules. Above figures in caption shows the cathode nBTMS interface (excluding amorphous polyethylene for better understanding of MNL thickness).

Table 2.2 nBTMS system thermal properties from MD simulations.

	nBTMS 10	nBTMS 20	nBTMS 30
Heat Flux (W/m^2)	2211797366.44	1537213431.72	1880415860.19
Temperature drop at interface (K)	20.19	12.01	13.46
Interfacial Thermal Conductance (W/m^2K)	109532799.043	128044743.344	139710395.378

In this system nBTMS molecules i.e., (n-Butyl trimethoxy silane) were used. nBTMS molecules have two functional sites on there each end, one is silane group and other end with methyl group. From the results shown below, there was not a significant improvement in the interfacial thermal conductance in the all three cases, only with 20 and 30 molecules shows slight amount of percentage improvement of 2.6% and 11.9% in the interfacial thermal conductance with respect to the pristine interface with no nBTMS molecules at the interface. One reason for this slight improvement was the end group functional sites of nBTMS molecules, other than the silane, one end was with the methyl group and the separator i.e. amorphous polyethylene have the same molecules [-CH3-] group, resulted in negligible affinity towards the methyl end and amorphous polyethylene, whereas silane group was well attracted towards the LiCoO2 and hence contributing in the nutshell improvement in interfacial thermal conductance.

3.2.3 Effect of MPTMS Molecules on cathode-separator interface:

For this system MPTMS molecule of 10/20 and 30 were used in between the cathode-separator interface. MPTMS molecules was very similar compare to the APTES molecules but having the [-SH-] termini at one end while silane group attached to methyl on the other end. Compare to nBTMS molecules it does have affinity towards LiCoO2 and amorphous polyethylene [-CH3-] group, because of the dissimilar end groups. By observing the following results, the MPTMS molecules showed the improvement in the interfacial thermal conductance of 11%, 174% and 11.3% for 10, 20 and 30 molecules respectively with pristine interface conductance.

Table 3.3 MPTMS system thermal properties from MD simulations

	MPTMS 10	MPTMS 20	MPTMS 30
Heat Flux (W/m^2)	2098345137	2062251163	1625900654
Temperature drop at interface (K)	15.1988392	6.0233968	11.7079124
Interfacial Thermal Conductance (W/m^2K)	138059565.6	342373453.3	138871952.4

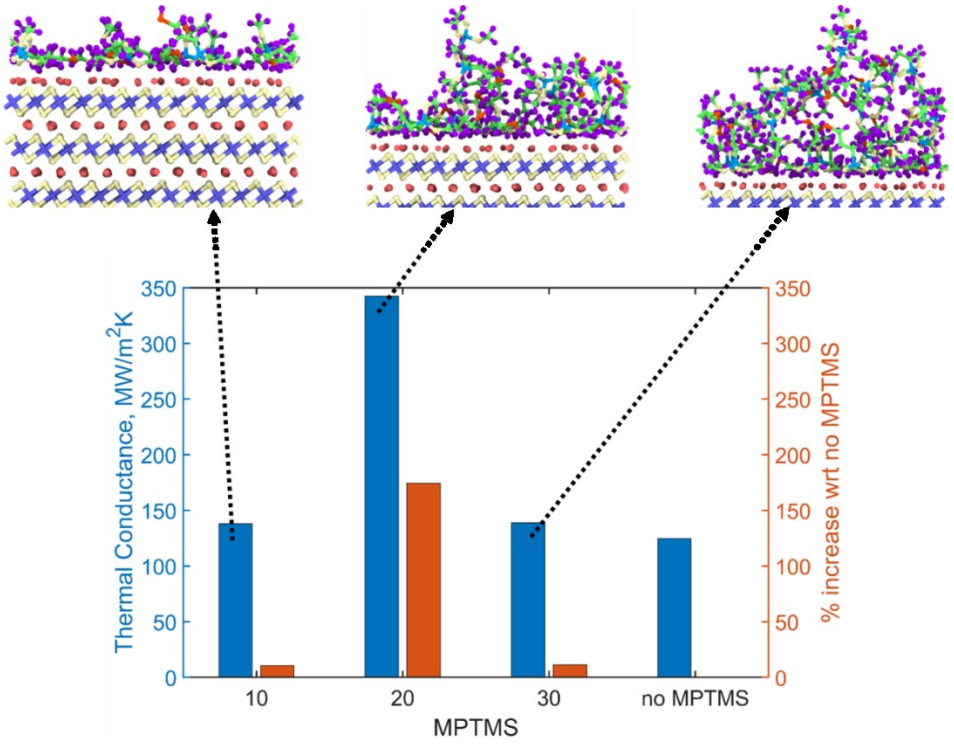

Figure 3.4 Shows the comparative results with increase in the number of molecules 10/20/30 MPTMS (blue-right) while the (orange-left) represent the percentage increase in the interfacial thermal conductance with respect to the pristine interface have no MPTMS.

3.3 Effect of Pressure:

While observing above results with functionalizing the interface, few void spaces in the MNL-amorphous polyethylene were observed. So the two system nBTMS 20/30 molecules were selected to study the effect of pressure. System were relaxed at 100 bar pressure and the NEMD was performed.

3.3.1 nBTMS 20 molecules:

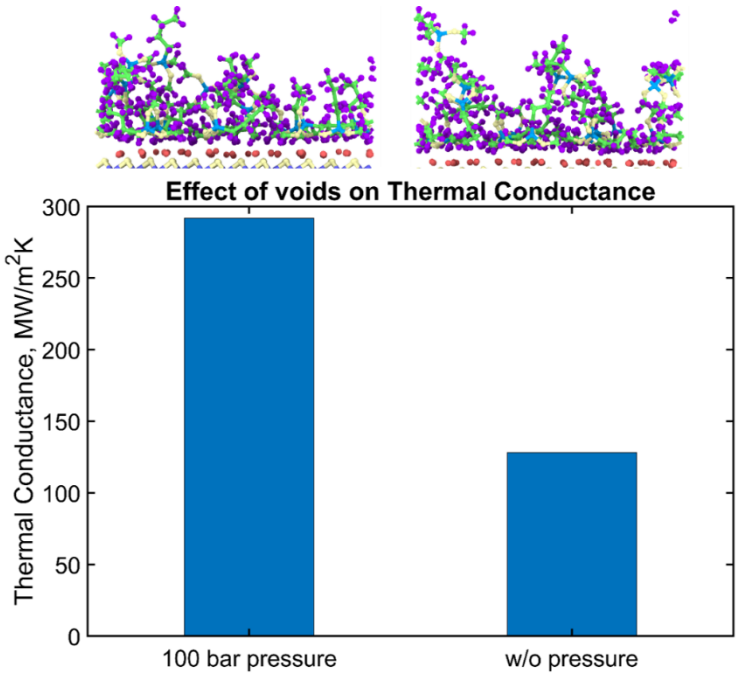

Figure 3.5 Shows the interfacial thermal conductance improvement after application of the 100 bar pressure along the elongated direction (z) compare with without pressure with interface having 20 nBTMS molecules.

Fig. (3.5) shows the results with and without 100 bar pressure with the interfacial thermal conductance. By applying 100 bar pressure the system size was observed to decreased by 4-6 A leads to minimum voids in the system and hence the improvement in the areal density at the interface. As contact at the interface improves, so as the thermal conductance. By comparing both results the thermal conductance improved by a 2X compare to without pressure.

3.3.2 nBTMS 30 molecules:

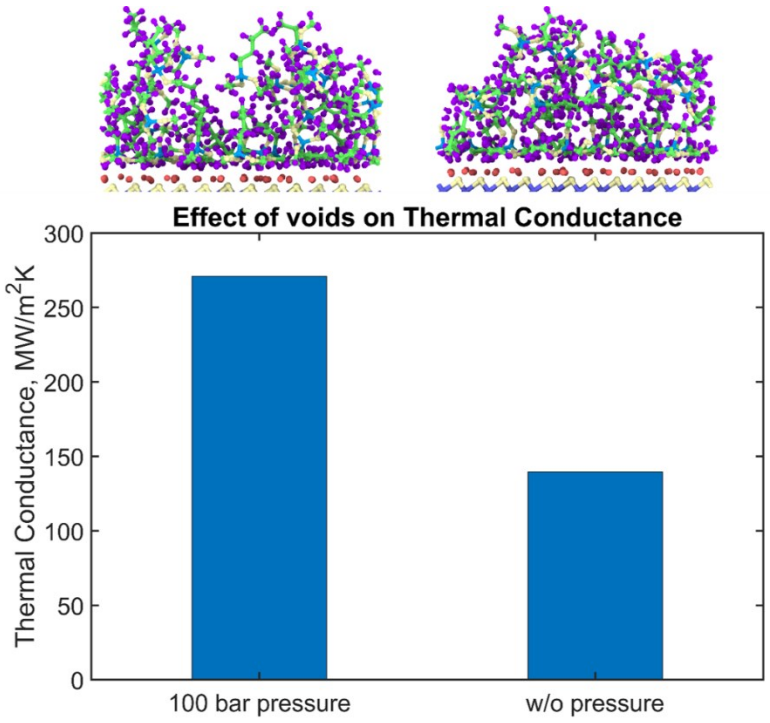

Figure 3.6 Shows the interfacial thermal conductance improvement after application of the 100 bar pressure along the elongated direction (z) compare with without pressure with interface having 30 nBTMS molecules.

Similar trend also observed in the above results depicted in fig(3.6). With the application of 100 bar pressure in the elongated direction decreases the void spaces in the system and hence leads to the improvement in the interfacial contact as well thermal conductance.

CHAPTER 4

DISCUSSION

After observing all the results and data. Few conclusions have been drawn. End group chemistry plays a very important role in the improvement in the interfacial thermal conductance. The molecules having affinity groups at their ends like [-NH2-] and [-SH-] shows very impressive results as both functional groups have an attraction towards the organic molecules [-CH3-] group. While on the other side the silane group was well attracted towards the metal oxides i.e., LiCoO2. Moreover, by increasing the number of molecules does not result in linear trend of improve interfacial thermal conductance because at some point it reached the saturation and it starts to add as a resistance to the system and therefore deteriorate the overall effect.

CHAPTER 5

FUTURE PLAN

We were planning to study the pressure effect of the other system which were not studied yet like APTES and MPTMS 20/30 molecules. By analyzing those results, it will be very helpful to down select the minimum number of molecules at the interface for the improved interfacial thermal conductance.

MNL molecules plays key role in improving the interfacial thermal conductance. So it will be important to study their thermal properties alone to know the mechanism behind the improved interfacial thermal conductance.

By trying different MNL molecules will help to improve the selection procedure for the MNL molecules for the actual experimental study. Rather than performing trial-error methods to efficiently select the performing candidate for the interface MNL.